SEMARAK ILMU PUBLISHING

CFD Letters

Journal homepage:
https://semarakilmu.com.my/journals/index.php/CFD_Letters/index
ISSN: 2180-1363

Computational Fluid Flow Model for the Development of an Arterial Bypass Graft

Hashem Shatnawi[1,*]

[1] Royal Commission for Jubail, Education Sector in Jubail, Jubail Technical Institute, Jubail Industrial City, 31961, Saudi Arabia

ARTICLE INFO

Article history:
Received 2 September 2022
Received in revised form 24 September 2022
Accepted 16 October 2022
Available online 31 October 2022

Keywords:
COMSOL; Blood flow; Coronary artery bypass graft; Dimensionless pressure drop

ABSTRACT

Intimal hyperplasia, an aberrant proliferation of smooth muscle cells that causes stenosis and graft occlusion, is the primary cause of the failure of grafts after a few years. In this way, and using the constructal design method, this study looks at how the stenosis degree, junction angle, and diameter ratio affect the flow through a bypass graft that goes around an idealised coronary artery partially blocked. The results show that the flow effect by several factors: Stenosis ratio (S), Bypass Attachment Point (L2), Bypass Angle (α), and Bypass Diameter (D1). The results indicate that the pressure drop is reduced when S is low, the optimal attachment point L2 = 4 Artery diameter (D), the optimal angle α = 30°, and the optimal D1 = 1.25D.

1. Introduction

When fat builds up in the walls of the arteries, it can partially or entirely block the flow of blood and lead to atherosclerosis, which is when the walls of the arteries get stiff [1-3]. Most heart attacks and strokes, especially in the West, are caused by atherosclerosis. Because of the buildup of lipids (like low-density lipoproteins, or LDL) in the intima, this disease causes the lumen to narrow and the artery wall to harden over time [4-7].

Newtonian fluids are fluids that obey the Newtonian law of viscosity [8]. However, a non-Newtonian fluid model has a non-linear relationship between shear stress and shear rate [9]. Examples of non-Newtonian liquids are polymer solution, ketchup, paint, colloids gel, custard, starch suspension, molten polymer, toothpaste shampoo, and blood [10]. Caro *et al.,* [11] investigated the overall distribution of wall shear across the arterial system at a specific Reynolds number, assuming the flow was steady and the arteries were rigid. The blood was a Newtonian fluid: The shear speeds up mass transport by making the concentration gradient steeper, which makes diffusion happen more quickly. Cholesterol transport between arterial walls and intraluminal blood depends on the shear.

Impiombato *et al.,* [12] examined the relationship between flow resistance and the location of the artery bypass graft placement using a 3D numerical model of an idealised graft. A steady-state

* *Corresponding author.*
E-mail address: Hashem121@yahoo.com (Hashem Shatnawi)

https://doi.org/10.37934/cfdl.14.10.99111

Newtonian fluid flow of 150, 250, and 400 Reynolds numbers are assumed in the computational model. The constructal theory was used in this investigation. They found a relationship between pressure drop and the distance between the bypass attachment point and the stenosis, with the pressure drop decreasing as the distance increases. The influence on the phase becomes nearly undetectable as the degree of stenosis increases. This means that as the flow is significantly diverted through the bypass, the impact on the phase decreases. D1/D equals 1, and 30° was the optimal point in both instances. This result suggested that a better outcome may be attained by raising the aspect ratio D1/D and decreasing the angle.

Dutra *et al.,* [13] utilised the Constructive Design Method with two degrees of freedom: the ratio of bypass to artery diameters and the junction angle at the bypass inlet. The flow problem was numerically solved using the Finite Volume Method, with blood viscosity represented using the Carreau equation. The Computational Fluid Dynamics model coupled with the Sparse Grid method generated eighteen response surfaces, each representing a severe stenosis degree of 75% for particular combinations of rheological parameters, dimensionless viscosity ratio, Carreau number, and flow index at two distinct Reynolds numbers, 150 and 250. Non-Newtonian rheological parameters had no effect on either the form of the response surfaces or the best bypass architecture, which comprised of a diameter ratio of 1 and a junction angle of 30°. However, the viscosity ratio and flow index significantly affected pressure drop, recirculation zones, and wall shear stress. The recirculation zones downstream of stenosis, where intimal hyperplasia is more widespread, were likewise impacted by rheological parameters.

Ko *et al.,* [14] found that in the host artery, axial recirculation was identified in all occluded cases and the distribution regions of recirculation zones grew as the stenosed severity rose. The secondary flow structures obviously occurred in the bypass graft for all stenosed patients, and the strength of secondary vortices increased with the stenosed degree. The percentage of the flow rate bifurcating into the bypass graft increased as the stenosed severity. The relationship between the percentage and the occlusion degree is essentially linear. The magnitudes, as well as the distributions of shear stress on arterial walls, were considerably altered by the stenosed severity of the host artery.

2. Methodology

2.1 Problem Design

The artery is represented by a host artery with a diameter of D, and a length of L. Stenosis lowers the diameter of the main tube to D_0. In the axial direction, the geometry is symmetric across the stenosis's centre. The graft is positioned L_2 from the stenosis's centre, and its diameter is represented by D_1. L_3 is the distance from the centre at which the stenosis starts. Figure 1 shows the precise placements of the inner, outer, and sidewalls. The flow problem involves a fluid that enters the domain with average velocity U_m at the tube inlet. Depending on flow conditions and geometric arrangement, a portion of the flow may be diverted to the bypass. The tube walls are solid, impermeable, and nonslip. In addition to these characteristics, it is presumed that the flow is two-dimensional, steady, incompressible, and laminar. Figure 1 shows the full computational model for the geometry, with main tube extensions of 25 diameters (L_5 = 25D and L_6 = 25D) to get a fully developed flow. At the inlet, a uniform velocity profile of U_m was applied. As a boundary condition, a pressure outlet was imposed at the Exit. The host arterial diameter D is identical to 3 mm in all simulations, comparable to the average value of the right coronary artery.

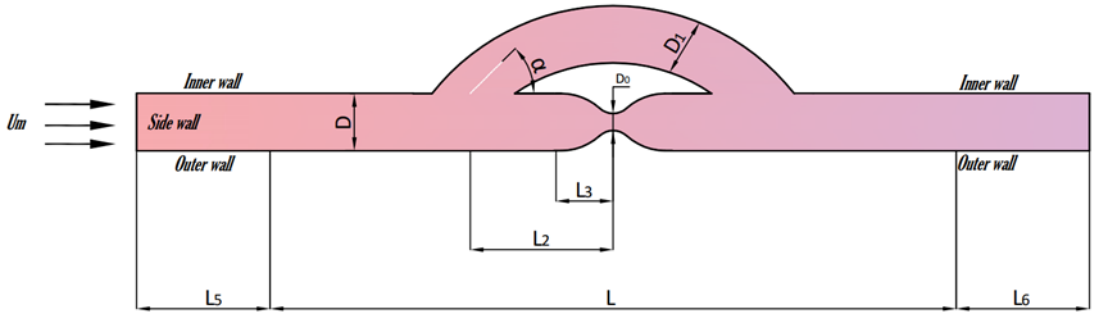

Fig. 1. A schematic diagram of the problem represented

Where:
D Artery Diameter, D_0 Stenosis Diameter, D_1 Bypass Diameter, *L* Measuring Length, L_1 Bypass Region, L_2 Bypass Attachment Point, L_3 Stenosis Beginning, L_4 Bypass Length, L_5 Added Length, and α Bypass Angle.

The stenosis degree S is calculated as in Eq. (1):

$$S = \frac{D-D_0}{D} \times 100\% \tag{1}$$

the pressure drop (ΔP) has been calculated as shown in Eq. (2)

$$\Delta P = \text{Pin} - \text{Pout} \tag{2}$$

2.2 Governing Equations

The flow system is described by the mass and moment balance Eq. (3) to (6) [2]:

$$\frac{\partial \tilde{u}_i}{\partial \tilde{x}_i} = 0 \tag{3}$$

$$\hat{u}_i \frac{\partial \tilde{u}_i}{\partial x_j} = -\frac{\partial \tilde{p}}{\partial \hat{x}_i} + \frac{1}{\text{Re}} \frac{\partial \bar{t}_{ij}}{\partial x_j} \tag{4}$$

$$\tilde{u}_i = \frac{u_i}{U_m}; \tilde{x}_i = \frac{x}{D}; \tilde{p} = \frac{\Delta p}{\rho U_m^2}; \tilde{\tau} = \frac{\tau_{ij}}{(U_m \mu)/D}; \ \text{Re} = \frac{\rho U_m D}{\mu} \tag{5}$$

$$\tau_{ij} = 2\eta(\dot{\gamma}) D_{ij} \tag{6}$$

2.3 Grid Indecency

For the grid independence study, different element sizes were chosen in COMSOL Multiphysics Software version 5.6 [15] to find the pressure difference along the distance L. the extra fine mesh was chosen with 250541 elements where the relative error was 0.18%, as shown in Table 1. The mesh is applied to the domain appearing in Figure 2.

Table 1
Grid independence study

Element size	No of elements	$\Delta P[Pa]$
Coarser	7511	169.89
Normal	20722	159.59
Fine	93728	148.58
Extra fine	250541	148.3
Extremely fine	329207	148.3

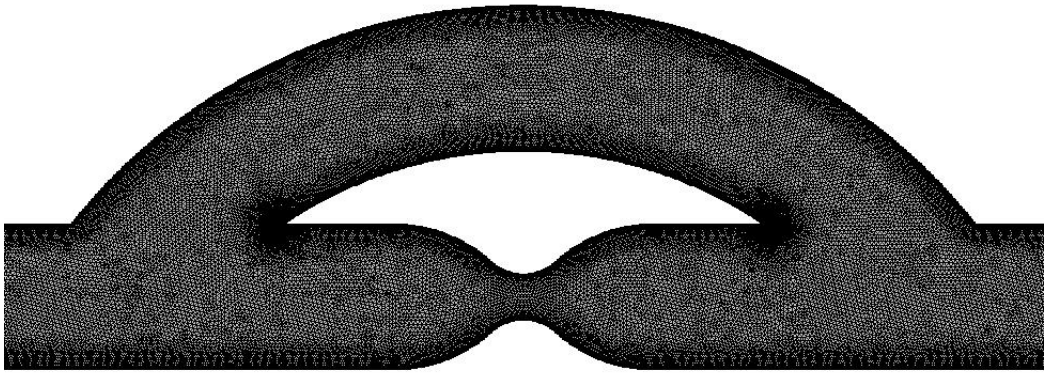

Fig. 2. Meshing applied to the domain

In order to verify the findings, a comparison was carried out [1,4] to determine the shear stress on the outer wall's surface. for the case of Reynolds number Re = 250, blood viscosity μ= 0.0035 kg/m.s, blood density ρ = 1000 kg/m^3 and the parameters of the arterial graft D1/D = 1, junction angle α = 45°, and stenosis degree S = 70%. Figure 3 shows the velocity contours of the validation case. As shown in Figure 4, there was a good match between the present results and the literature on shear stress calculations.

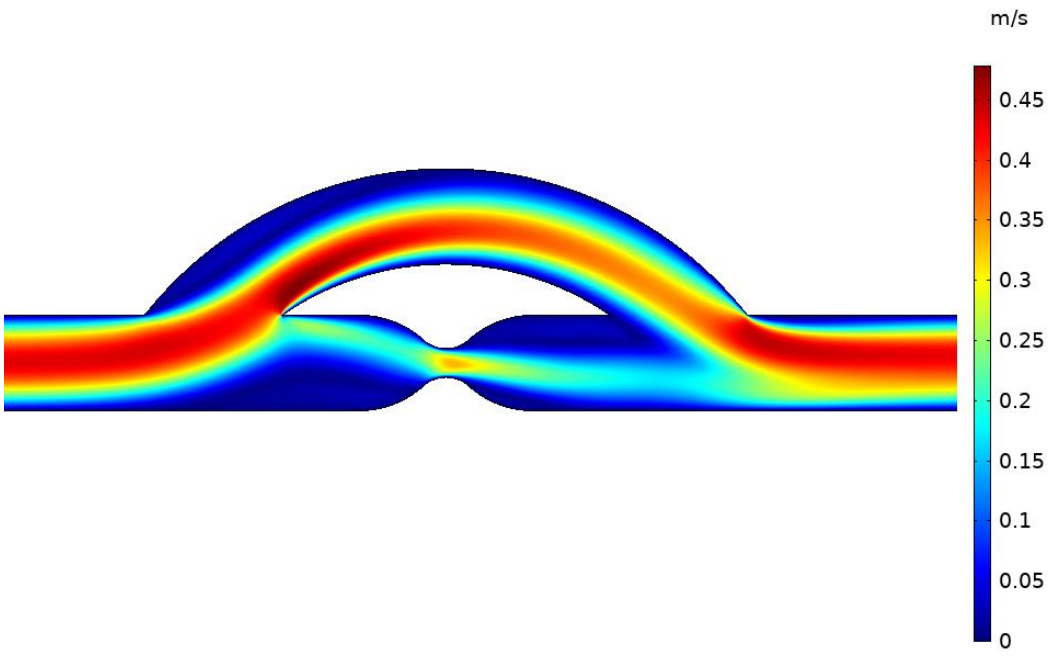

Fig. 3. Velocity contours of the validation model

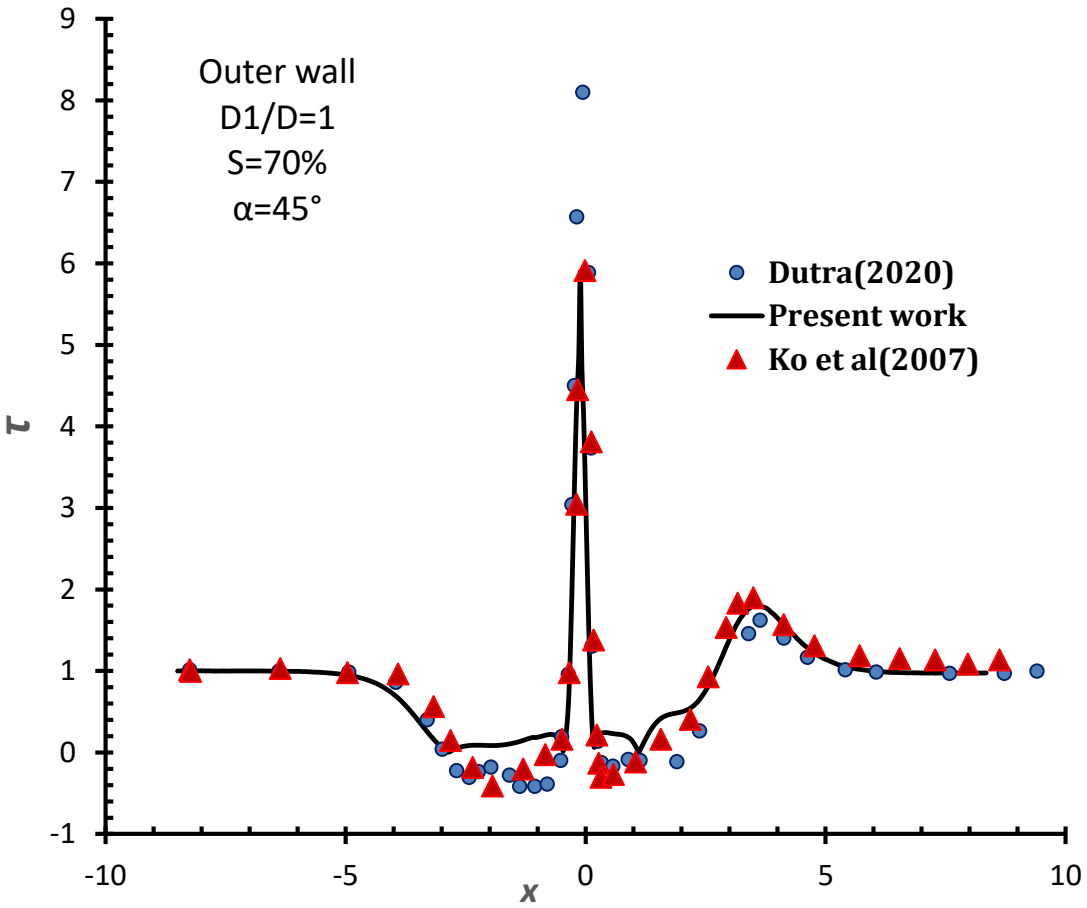

Fig. 4. Model verification, $D_1/D=1$, S=70%, α=45° (outer wall)

3. Result and Discussion

The work focuses on changing the bypass attachment point L_2 to study the effect of the place attachment position before stenosis and how much it affects the velocity and the pressure drop when increasing L_2.

To find the proper ratio of L_2/D a comparison has been made between the same parameters with L_2/D= 2.5 and 3. Table 2 presents the parameters chosen to represent the first possible scenario. Figure 5 shows a visual representation of the shear forces that are present along the out wall for various Reynolds values. After the stenosis, an increase in the Re causes an increase in the shear stress, whereas before the stenosis, an increase in the Re causes a drop in the shear stress.

Table 2
First case parameters

Re	α	D_1/D	S	L_2/D (from left)
50,150,250,400,500	45	1	0.7	2.5

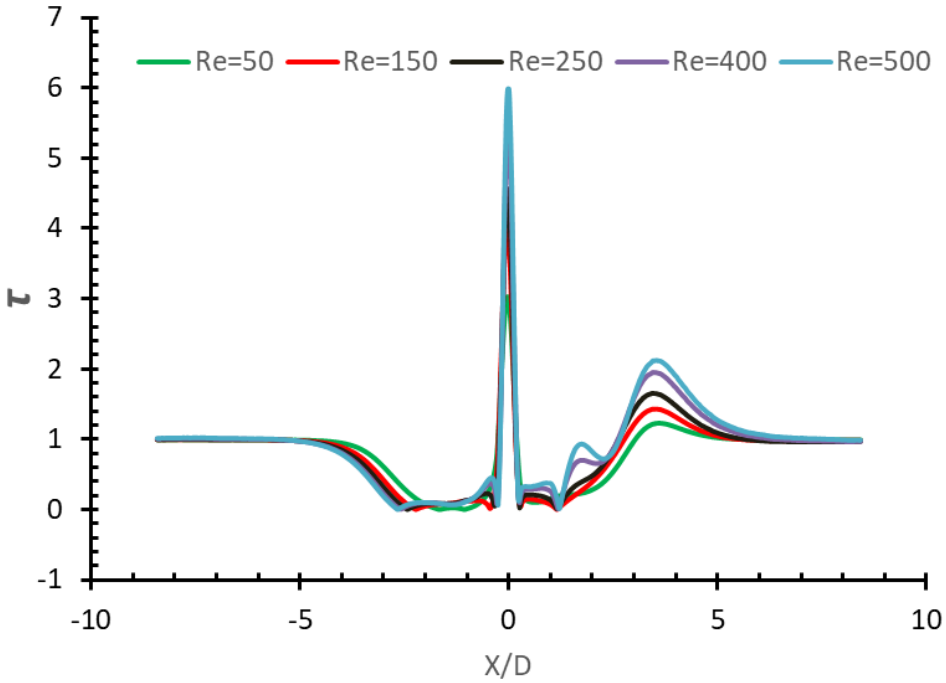

Fig. 5. Shear stresses with different Re at the outer wall

Figure 6 represent the velocity contour with different Reynolds number; while the pressure drop is small with a low Reynolds number, it is clear that the pressure drop increases with increasing Re; the Pressure drop reaches 50% with Re=500m and 39% at Re=50.

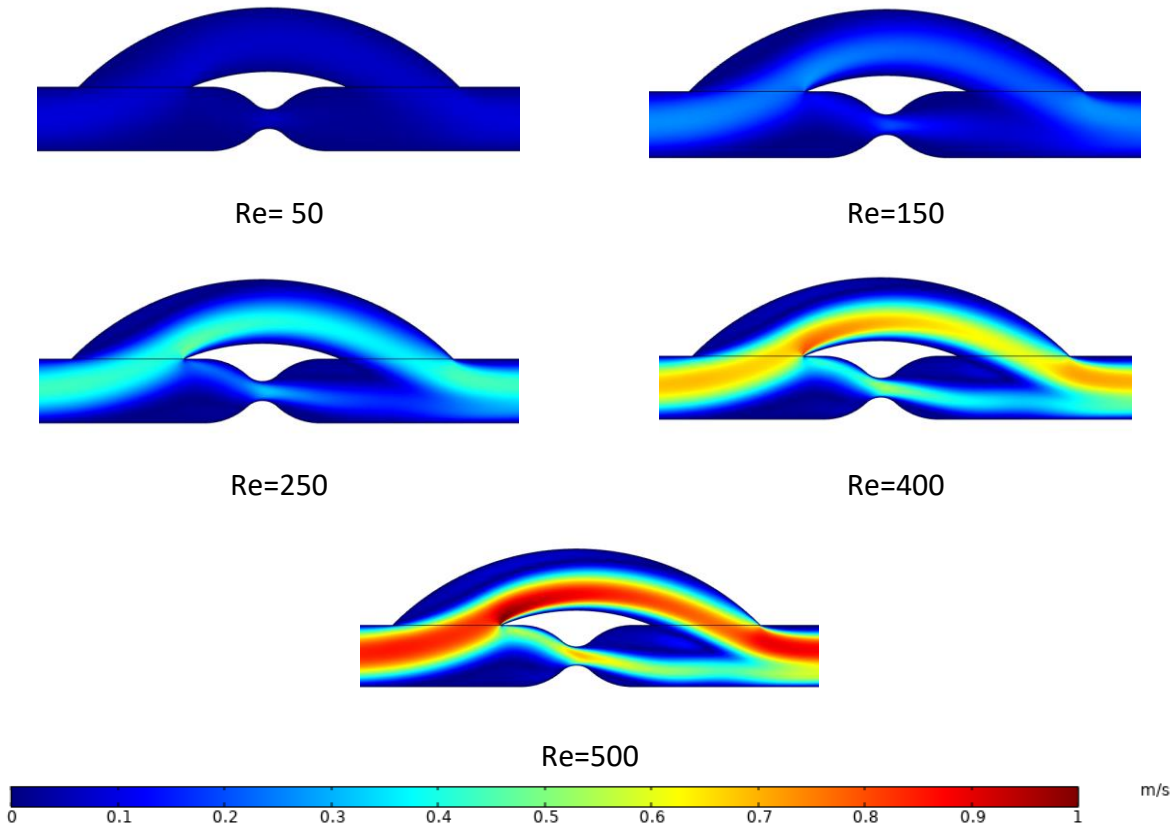

Fig. 6 Velocity contours with different Reynolds numbers at α=45°

As seen in Figure 7, the shear stress on the inner wall rises with increasing Re before the stenosis and reaches its maximum value in the stenosis zone when Re is at its highest value.

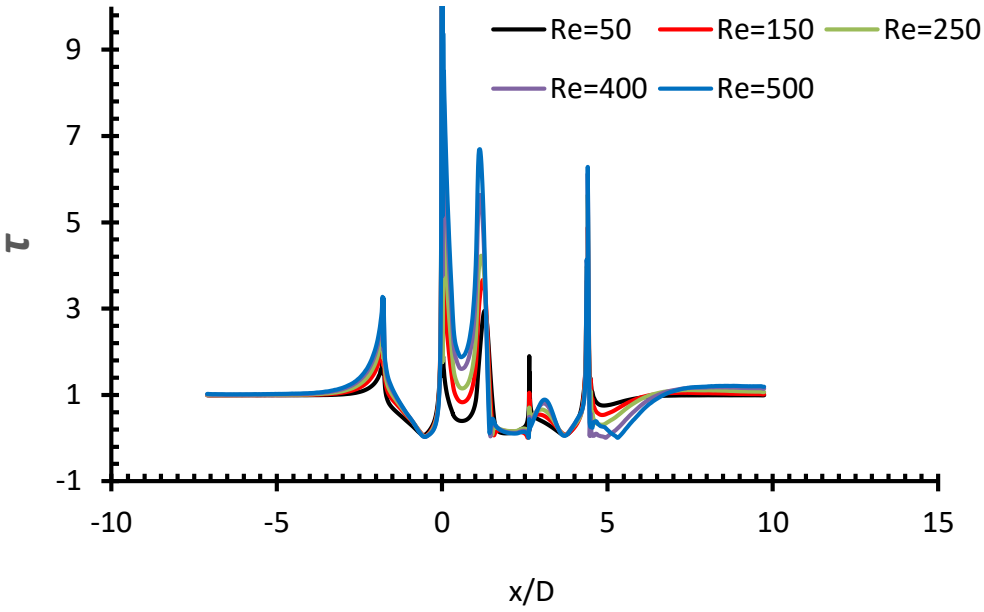

Fig. 7. Shear stresses with different Re at the inner wall

For L_2/D =3, the parameters selected for the second probable scenario are shown in Table 3. The bypass attachment point length increased to 3D. Figure 8 illustrates the velocity contours for Re=250. The pressure drop ratio is 45.3%.

Table 3
Second case parameters

Re	α	D_1/D	S	L_2/D (from left)
50,150,250,400,500	45	1	0.7	3

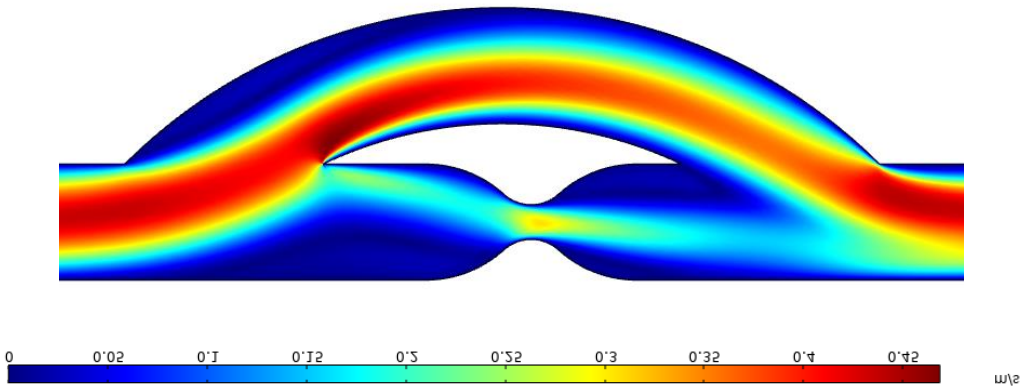

Fig. 8. Velocity contours at Re=250 and L_2=3D, D_1/D=1.

The pressure drop when L_2/D= 3 is equal to 45%, which is less when L_2/D=2.5, so further investigation is carried out with L_2/D=3

3.1 Effect of Bypass Diameter

The bypass diameters selected are 0.5, 0.75, 1, and 1.25. For the ratio D_1/D equal to 0.5, L_2/D=3, S=0.7, and α=45°. The pressure drop ratio increased dramatically with decreasing the bypass diameter. The pressure drop for the reference case is ΔP_1 and $\Delta P^* = \Delta P / \Delta P_1$. In Figure 9, it is clear that as the ratio D_1/D decreases the pressure drop increases, the pressure drop is 180% when Reynolds 50 for the ratio D_1/D=0.5 and it is reached 200% near Reynolds number 250 for the same ratio. When D_1/D=1.0, the pressure drop remains constant with a slight decrease up to 1.2% near Reynolds number 250.

Increasing the bypass diameter provides better performance with less pressure drop when D_1/D=1.25 As a result, decreasing the ratio of D_1/D increases the pressure drop. Figure 10 represents the velocity contours for the selected case.

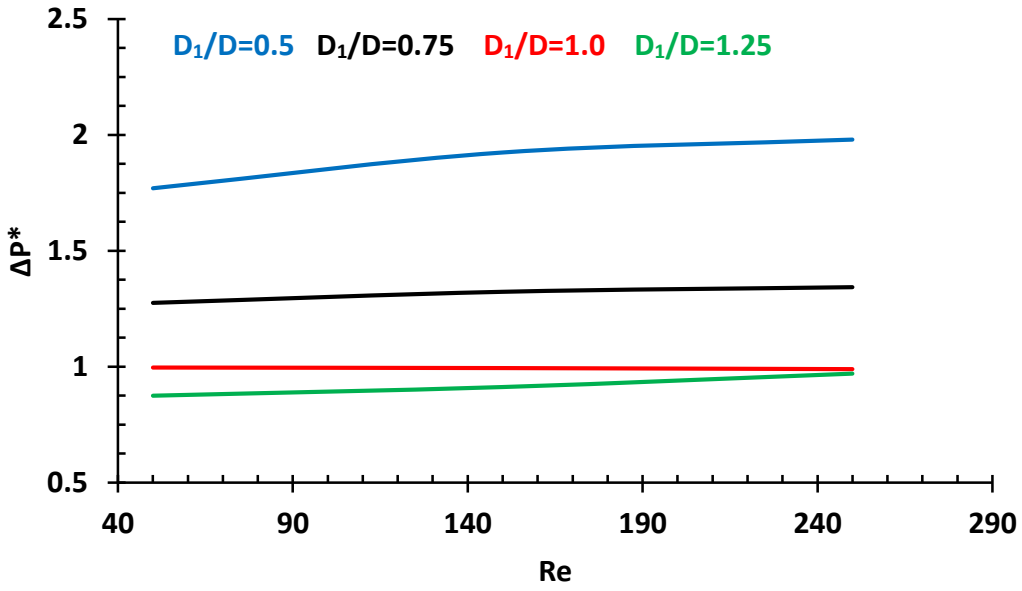

Fig. 9. Pressure drop with different Re, with different bypass diameter

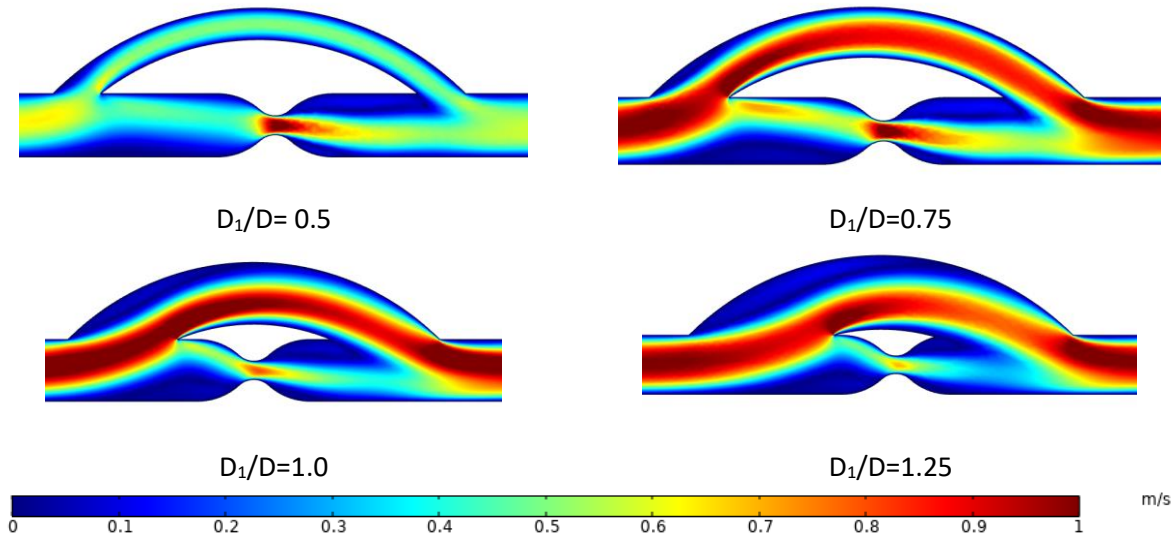

Fig. 10. Velocity contours with different D_1/D ration with Re=250 and α=45°

3.2 Effect of Bypass Angle

Three values of α were considered 30^0, 45^0, and 70^0. it is clear that the pressure drop increases as α increases. Moreover, the best angle that provides less drop in pressure is 30^0 by 12% compared with the reference case, as illustrated in Figure 11. The velocity contours are displayed in Figure 12.

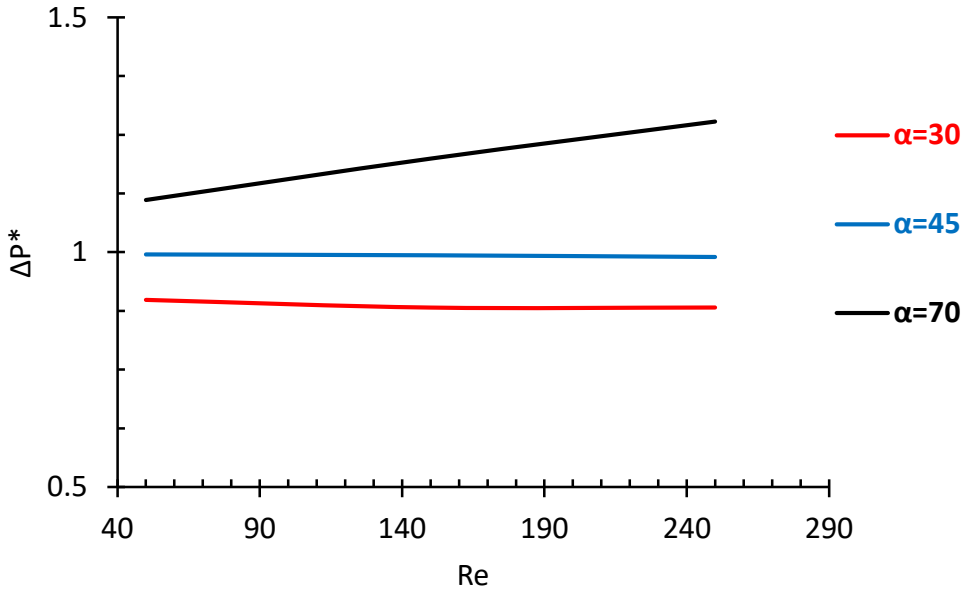

Fig. 11. Pressure drop ration different α, at $D_1/D=1$ and Re=250

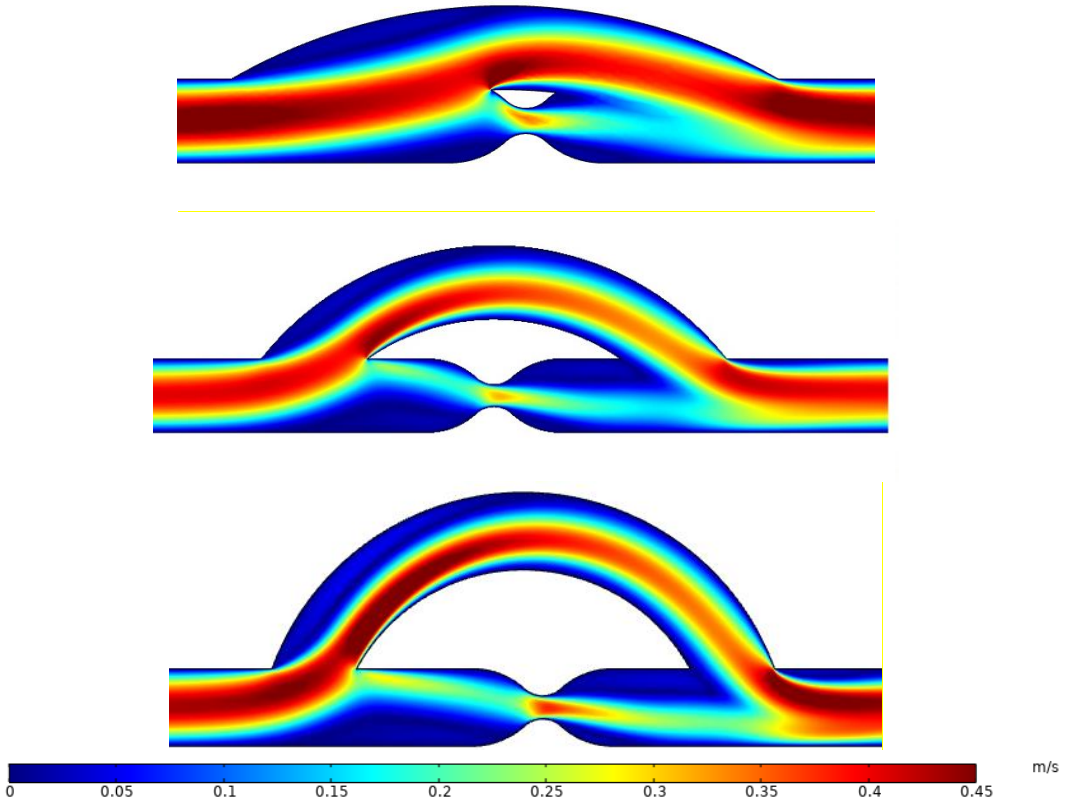

Fig. 12. Velocity contours with α=30°, 45°, 70°, at $D_1/D=1$ and Re=250

3.3 Effect of Bypass Attachment Point

To study the effect of increasing the entrance length when $\alpha=30^0$ and S=0.7, the result was compared with a reference case where $\alpha=45^0$, S=0.7, and $L_2/D=2.5$. As the ratio L_2/D increases the pressure drop decreases until it reaches the optimized ratio ($L_2/D=4$) and then starts to rise again when L2/D=5, as shown in Figure 13. The velocity contours illustrate in Figure 14.

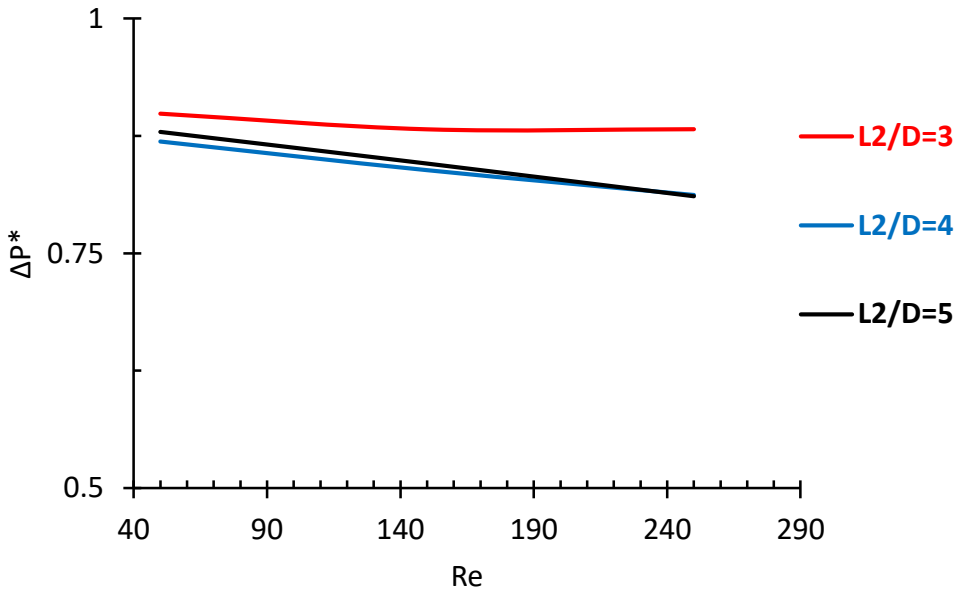

Fig. 13. Pressure drop ratio with different L_2, when α=30°, at $D_1/D=1$ and Re=250

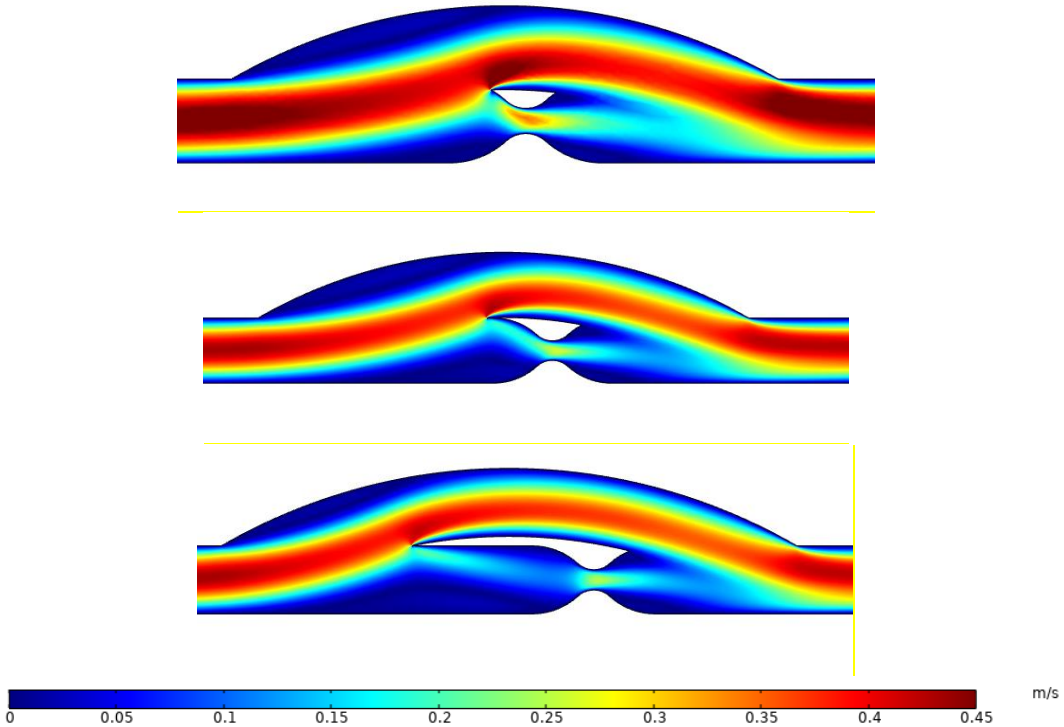

Fig. 14. Velocity contours with L_2/D=3,4, and 5, when α=30°, at $D_1/D=1$ and Re=250

3.4 Effect of Stenosis Ratio

An investigation into the influence of stenosis size was carried out in this case when the values of S were selected as 0.25, 0.5, and 0.75. When the S value is high, the pressure drop is significant; when the S value is low, the pressure drop is smaller, as illustrated in Figure 15. The velocity contours are shown in Figure 16.

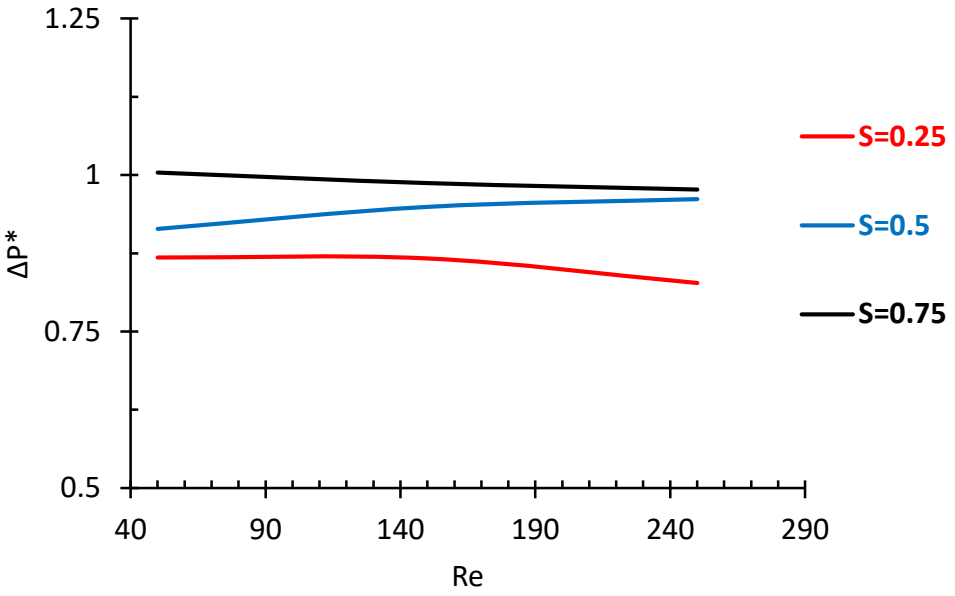

Fig. 15. Pressure drop with different S, when α= 45°, at D_1/D=1, L_2/D=4, and Re=250

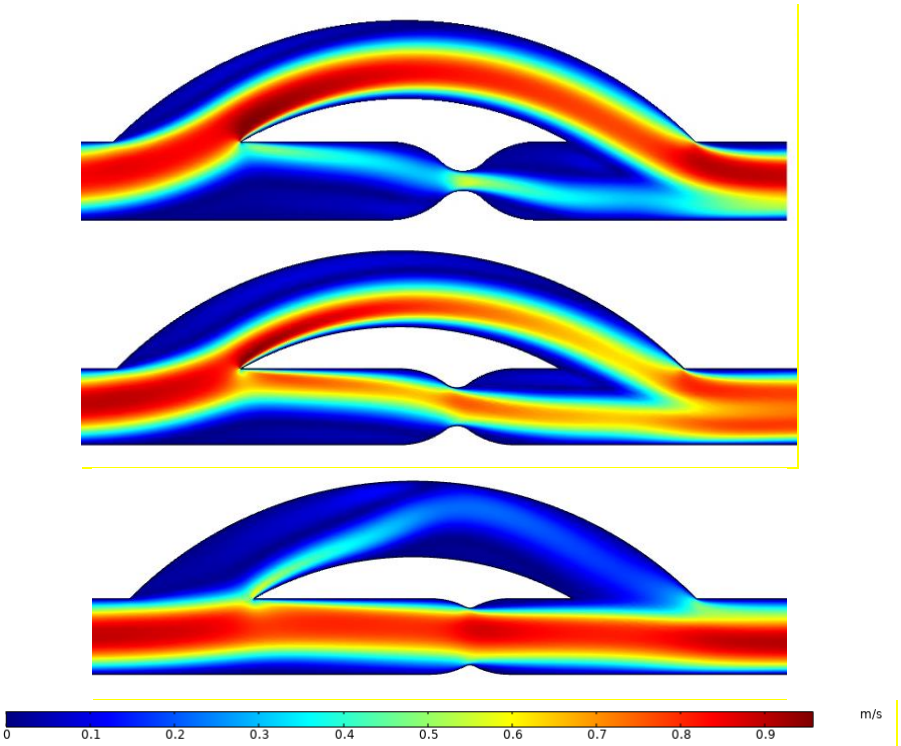

Fig. 16. Velocity contours of S=0.25, 0.5, 0.75, when α= 45°, at D_1/D=1, L_2/D=4, and Re=250

4. Conclusion

This study examined the impacts of geometric parameters on the various flow of a bypass graft in an idealised coronary artery with partial stenosis. In order to simulate the behaviour of the numerical model, version 5.6 of the COMSOL Multiphysics software was utilised. The results indicate that the pressure drop is reduced when the stenosis ratio S =0.25, the optimal attachment point L_2 = 4D, the optimal angle α = 30°, and the optimal D_1 = 1.25D.

References

[1] Cameron, A., H. G. Kemp, and G. E. Green. "Internal Mammary Artery Grafts, 15 Years Clinical Follow-Up." In *Circulation*, vol. 72, no. 4, pp. 293-293. 7272 Greenville Avenue, Dallas, Tx 75231-4596: Amer Heart Assoc, 1985.

[2] Dutra, Rafael F., Flavia SF Zinani, Luiz AO Rocha, and C. Biserni. "Constructal design of an arterial bypass graft." *Heat Transfer* 49, no. 7 (2020): 4019-4039. https://doi.org/10.1002/htj.21693

[3] Fischman, David L., Martin B. Leon, Donald S. Baim, Richard A. Schatz, Michael P. Savage, Ian Penn, Katherine Detre et al. "A randomized comparison of coronary-stent placement and balloon angioplasty in the treatment of coronary artery disease." *New England Journal of Medicine* 331, no. 8 (1994): 496-501. https://doi.org/10.1056/NEJM199408253310802

[4] Hegde, Pranav, SM Abdul Khader, Raghuvir Pai, Masaaki Tamagawa, Ravindra Prabhu, Nitesh Kumar, and Kamarul Arifin Ahmad. "CFD Analysis on Effect of Angulation in A Healthy Abdominal Aorta-Renal Artery Junction." *Journal of Advanced Research in Fluid Mechanics and Thermal Sciences* 88, no. 1 (2021): 149-165. https://doi.org/10.37934/arfmts.88.1.149165

[5] Tian, Fang-Bao, Luoding Zhu, Pak-Wing Fok, and Xi-Yun Lu. "Simulation of a pulsatile non-Newtonian flow past a stenosed 2D artery with atherosclerosis." *Computers in biology and medicine* 43, no. 9 (2013): 1098-1113. https://doi.org/10.1016/j.compbiomed.2013.05.023

[6] Giddens, D. P., C. K. Zarins, and S. Glagov. "Response of arteries to near-wall fluid dynamic behavior." (1990): S98-S102. https://doi.org/10.1115/1.3120861

[7] Politis, A. K., G. P. Stavropoulos, M. N. Christolis, F. G. Panagopoulos, N. S. Vlachos, and N. C. Markatos. "Numerical modeling of simulated blood flow in idealized composite arterial coronary grafts: Steady state simulations." *Journal of Biomechanics* 40, no. 5 (2007): 1125-1136. https://doi.org/10.1016/j.jbiomech.2006.05.008

[8] Yusof, Nur Syamila, Siti Khuzaimah Soid, Mohd Rijal Illias, Ahmad Sukri Abd Aziz, and Nor Ain Azeany Mohd Nasir. "Radiative Boundary Layer Flow of Casson Fluid Over an Exponentially Permeable Slippery Riga Plate with Viscous Dissipation." *Journal of Advanced Research in Applied Sciences and Engineering Technology* 21, no. 1 (2020): 41-51. https://doi.org/10.37934/araset.21.1.4151

[9] Zin, Ahmad Faiz Mat, Ishkrizat Taib, Muhammad Hanafi Asril Rajo Mantari, Bukhari Manshoor, Ahmad Mubarak Tajul Arifin, Mahmod Abd Hakim Mohamad, Muhammad Sufi Roslan, and Muhammad Rafiuddin Azman. "Temperature Variation with Hemodynamic Effect Simulation on Wall Shear Stress in Fusiform Cerebral Aneurysm." *Journal of Advanced Research in Fluid Mechanics and Thermal Sciences* 95, no. 2 (2022): 40-54.https://doi.org/10.37934/arfmts.95.2.4054

[10] Beleri, Joonabi, and Asha S. Kotnurkar. "Peristaltic Transport of Ellis Fluid under the Influence of Viscous Dissipation Through a Non-Uniform Channel by Multi-Step Differential Transformation Method." *Journal of Advanced Research in Numerical Heat Transfer* 9, no. 1 (2022): 1-18.

[11] Caro, C. G., J. M. Fitz-Gerald, and R. C. Schroter. "Atheroma and arterial wall shear-observation, correlation and proposal of a shear dependent mass transfer mechanism for atherogenesis." *Proceedings of the Royal Society of London. Series B. Biological Sciences* 177, no. 1046 (1971): 109-133. https://doi.org/10.1098/rspb.1971.0019

[12] Impiombato, A. N., F. S. F. Zinani, L. A. O. Rocha, and C. Biserni. "Pulsatile flow through an idealized arterial bypass graft: an application of the constructal design method." *Journal of the Brazilian Society of Mechanical Sciences and Engineering* 43, no. 8 (2021): 1-10. https://doi.org/10.1007/s40430-021-03048-8

[13] Dutra, R. F., F. S. F. Zinani, L. A. O. Rocha, and Cesare Biserni. "Effect of non-Newtonian fluid rheology on an arterial bypass graft: A numerical investigation guided by constructal design." *Computer Methods and Programs in Biomedicine* 201 (2021): 105944. https://doi.org/10.1016/j.cmpb.2021.105944

[14] Ko, T. H., Kuen Ting, and H. C. Yeh. "Numerical investigation on flow fields in partially stenosed artery with complete bypass graft: An in vitro study." *International communications in heat and mass transfer* 34, no. 6 (2007): 713-727. https://doi.org/10.1016/j.icheatmasstransfer.2007.03.010

[15] Shatnawi, Hashem, Chin Wai Lim, Firas Basim Ismail, and Abdulrahman Aldossary. "Numerical study of heat transfer enhancement in a solar tower power receiver, through the introduction of internal fins." *Journal of Advanced*

Research in Fluid Mechanics and Thermal Sciences 74, no. 1 (2020): 98-118. https://doi.org/10.37934/arfmts.74.1.98118